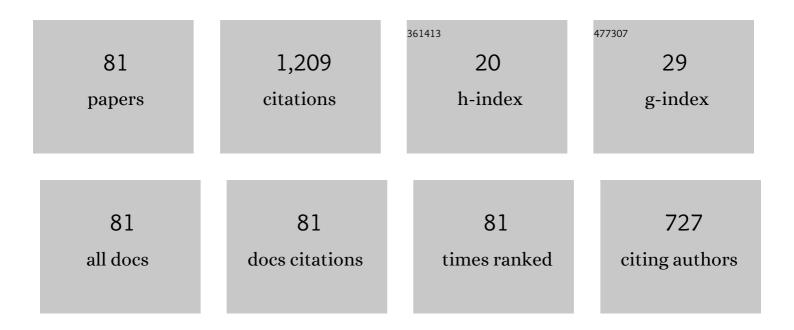


List of Publications by Year in descending order

Source: https://exaly.com/author-pdf/5052832/publications.pdf Version: 2024-02-01



XIAODO

#	Article	IF	CITATIONS
1	Effects of temperature and particles volume concentration on the thermophysical properties and the rheological behavior of CuO/MgO/TiO2 aqueous ternary hybrid nanofluid. Journal of Thermal Analysis and Calorimetry, 2019, 137, 879-901.	3.6	106
2	Experimental investigations of density and dynamic viscosity of n -hexadecane with three fatty acid methyl esters. Fuel, 2016, 166, 553-559.	6.4	53
3	Performance analysis of R1234yf/ionic liquid working fluids for single-effect and compression-assisted absorption refrigeration systems. International Journal of Refrigeration, 2020, 109, 25-36.	3.4	48
4	Measurement and correlation of density and viscosity of n -hexadecane with three fatty acid ethyl esters. Journal of Chemical Thermodynamics, 2016, 97, 127-134.	2.0	46
5	Densities and Viscosities of Binary Mixtures of 2,2,4-Trimethylpentane + 1-Propanol, + 1-Pentanol, + 1-Hexanol, and + 1-Heptanol from (298.15 to 323.15) K. Journal of Chemical & Engineering Data, 2015, 60, 1664-1673.	1.9	37
6	Volumetric and viscometric properties of ethyl caprate + 1-propanol, + 1-butanol, and + 1-pentanol from 283.15 K to 318.15 K. Journal of Molecular Liquids, 2017, 225, 311-319.	4.9	36
7	Gaseous absorption of 2,3,3,3-tetrafluoroprop-1-ene in three imidazolium-based ionic liquids. Fluid Phase Equilibria, 2017, 450, 65-74.	2.5	35
8	Accurate <i>ab initio</i> potential for the krypton dimer and transport properties of the low-density krypton gas. Journal of Chemical Physics, 2015, 142, 204307.	3.0	33
9	Experimental investigations on the liquid thermal conductivity of five saturated fatty acid methyl esters components of biodiesel. Journal of Chemical Thermodynamics, 2018, 125, 50-55.	2.0	29
10	Experimental investigations on the thermophysical properties of methyl myristate in alcoholic solutions. Fuel, 2018, 215, 187-195.	6.4	27
11	Vapor–Liquid Equilibria for R1234ze(E) and Three Imidazolium-Based Ionic Liquids as Working Pairs in Absorption–Refrigeration Cycle. Journal of Chemical & Engineering Data, 2018, 63, 3053-3060.	1.9	27
12	Density and viscosity for binary mixtures of methyl decanoate with 1-propanol, 1-butanol, and 1-pentanol. Journal of Molecular Liquids, 2019, 294, 111647.	4.9	27
13	Experimental investigation of wettability alteration of carbonate gas-condensate reservoirs from oil-wetting to gas-wetting using Fe3O4 nanoparticles coated with Poly (vinyl alcohol), (PVA) or Hydroxyapatite (HAp). Journal of Petroleum Science and Engineering, 2020, 184, 106530.	4.2	27
14	Measurement and correlation for phase equilibrium of HFO1234yf with three pentaerythritol esters from 293.15 K to 348.15 K. Journal of Chemical Thermodynamics, 2017, 112, 122-128.	2.0	25
15	Effect of Modified Fe ₃ O ₄ Magnetic NPs on the Absorption Capacity of CO ₂ in Water, Wettability Alteration of Carbonate Rock Surface, and Water–Oil Interfacial Tension for Oilfield Applications. Industrial & Engineering Chemistry Research, 2021, 60. 3421-3434.	3.7	25
16	Surface Tension of Dimethoxymethane and Methyltert-Butyl Ether. Journal of Chemical & Engineering Data, 2006, 51, 1394-1397.	1.9	24
17	High-pressure liquid densities and derived thermodynamic properties for methyl laurate and ethyl laurate. Journal of Chemical Thermodynamics, 2016, 103, 310-315.	2.0	22
18	Density, Viscosity, and Thermal Conductivity of Eight Carboxylic Acids from (290.3 to 473.4) K. Journal of Chemical & Engineering Data, 2016, 61, 2651-2658.	1.9	22

#	Article	IF	CITATIONS
19	Phase Equilibria of <i>trans</i> -1,3,3,3-Tetrafluoropropene with Three Imidazolium Ionic Liquids. Journal of Chemical & Engineering Data, 2017, 62, 1825-1831.	1.9	22
20	Gaseous solubility and thermodynamic performance of absorption system using R1234yf/IL working pairs. Applied Thermal Engineering, 2020, 172, 115161.	6.0	22
21	Influence of Aprotic Cosolvents on the Thermophysical Properties of Imidazolium-Based Ionic Liquid. Journal of Chemical & Engineering Data, 2017, 62, 1628-1638.	1.9	21
22	Vapor-liquid equilibrium of 2,3,3,3-tetrafluoroprop-1-ene with 1-butyl-3-methylimidazolium hexafluorophosphate, 1-hexyl-3-methyl imidazolium hexafluorophosphate, and 1-octyl-3-methylimidazolium hexafluorophosphate. Journal of Molecular Liquids, 2018, 260, 203-208.	4.9	21
23	Solubility of Dimethyl Ether in Pentaerythritol Tetrahexanoate (PEC6) and in Pentaerythritol Tetraoctanoate (PEC8) Between (283.15 and 353.15) K. Journal of Chemical & Engineering Data, 2014, 59, 3791-3797.	1.9	19
24	Solubility of trans-1,3,3,3-tetrafluoroprop-1-ene (R1234ze(E)) in pentaerythritol tetrapentanoate (PEC5) in the temperature range from 283.15 to 353.15ÅK. International Journal of Refrigeration, 2014, 48, 114-120.	3.4	19
25	Measurement on the thermal conductivity of five saturated fatty acid ethyl esters components of biodiesel. Fluid Phase Equilibria, 2018, 473, 106-111.	2.5	19
26	Experimental investigation for the solubility of R1234ze(E) in pentaerythritol tetrahexanoate and pentaerythritol tetraoctanoate. Fluid Phase Equilibria, 2015, 400, 38-42.	2.5	17
27	Effect of organic solvents on lowering the viscosity of 1-hexyl-3-methylimidazolium chloride. Journal of Chemical Thermodynamics, 2017, 113, 358-368.	2.0	17
28	Nanofluid viscosity modeling based on the friction theory. Journal of Molecular Liquids, 2019, 286, 110923.	4.9	17
29	Experimental studies on the liquid thermal conductivity of three saturated fatty acid methyl esters components of biodiesel. Journal of Chemical Thermodynamics, 2018, 125, 200-204.	2.0	16
30	Phase equilibrium of R1234yf and R1234ze(E) with POE lubricant and thermodynamic performance on the evaporator. Fluid Phase Equilibria, 2020, 514, 112562.	2.5	16
31	Modeling Hydrofluoroolefins with the Cubic Plus Association and Perturbed-Chain Statistical Associating Fluid Theory Equations of State. Industrial & Engineering Chemistry Research, 2018, 57, 17289-17300.	3.7	15
32	Experimental investigation on the solubility of R290 in two mineral oils. International Journal of Refrigeration, 2021, 124, 13-19.	3.4	15
33	Viscosity of saturated mixtures of 1-hexyl-3-methyl-imidazolium bis(trifluoromethylsulfonyl)amide with R600a and R152a. Journal of Chemical Thermodynamics, 2020, 141, 105970.	2.0	14
34	Recommended gas transport properties of argon at low density using <i>ab initio</i> potential. Molecular Simulation, 2016, 42, 9-13.	2.0	13
35	Experimental studies on the thermal conductivity of methyl laurate component of biodiesel with three alcohols. Journal of Chemical Thermodynamics, 2019, 139, 105881.	2.0	13
36	Liquid viscosities for methyl hexanoate, methyl heptanoate, methyl caprylate, and methyl nonanoate at high pressures. Journal of Chemical Thermodynamics, 2019, 133, 285-291.	2.0	13

#	Article	IF	CITATIONS
37	Active Frequency Tuning for Magnetically Actuated and Piezoresistively Sensed MEMS Resonators. IEEE Electron Device Letters, 2013, 34, 921-923.	3.9	12
38	Calculations of the thermophysical properties of binary mixtures of noble gases at low density from ab initiopotentials. Molecular Physics, 2011, 109, 1607-1615.	1.7	11
39	Solubility of dimethyl ether in pentaerythritol tetrabutyrate and in pentaerythritol tetrapentanoate. Comparison with other pentaerythritol tetraalkyl esters. Journal of Chemical Thermodynamics, 2015, 87, 23-28.	2.0	11
40	Densities of FAMEs or FAEEs with ethanol at temperatures from 283.15 to 318.15 K. Physics and Chemistry of Liquids, 2018, 56, 33-42.	1.2	11
41	Phase behavior of R1234yf and R600a in pentaerythritol tetranonanoate. International Journal of Refrigeration, 2020, 109, 135-142.	3.4	11
42	Absorption behavior for R1234ze(E) and R1233zd(E) in [P66614][Cl] as working fluids in absorption refrigeration systems. International Journal of Refrigeration, 2021, 131, 178-185.	3.4	11
43	Prior lactose glycation of caseinate via the Maillard reaction affects in vitro activities of the pepsin-trypsin digest toward intestinal epithelial cells. Journal of Dairy Science, 2017, 100, 5125-5138.	3.4	10
44	Volumetric Properties of 1-Butyl-3-methylimidazolium Chloride with Organic Solvents. Journal of Chemical & Engineering Data, 2017, 62, 3958-3966.	1.9	10
45	Solubility Measurement and Correlation of Isobutane with Two Pentaerythritol Tetraalkyl Esters between (293.15 and 348.15) K. Journal of Chemical & Engineering Data, 2015, 60, 1504-1509.	1.9	9
46	Densities and excess molar volumes of methanol with three fatty acid methyl esters from 283.15 to 318.15 K. Energy Procedia, 2018, 152, 143-148.	1.8	9
47	Measurements of the thermal conductivity of three pure alcohols and their binary mixtures with methyl myristate component of biodiesel. Journal of Chemical Thermodynamics, 2020, 142, 106009.	2.0	9
48	Experimental investigation on the viscosity of [Hmim][Tf2N] saturated with R1234ze(E) or R1234yf. International Journal of Refrigeration, 2020, 117, 338-345.	3.4	9
49	In-Situ Measurement of Fluid Density Rapidly Using a Vibrating Piezoresistive Microcantilever Sensor Without Resonance Occurring. IEEE Sensors Journal, 2014, 14, 645-650.	4.7	8
50	Viscosity Calculation for Binary Mixtures of Organic Solvents Based on Modified Eyring-Modified Two-Suffix-Margules (MTSM) Model. Journal of Chemical & Engineering Data, 2018, 63, 1382-1388.	1.9	8
51	Solubility for Propane and Isobutane in [P ₆₆₆₁₄]Cl from 278.15 to 348.15 K. Journal of Chemical & Engineering Data, 2021, 66, 1273-1279.	1.9	8
52	Solubility measurement, modeling and mixing thermodynamic properties of R1243zf and R600a in [BMIM][Ac]. Journal of Chemical Thermodynamics, 2022, 164, 106637.	2.0	8
53	Volumetric properties of n-hexadecane/ethyl octanoate mixtures from 293.15ÂK to 363.15ÂK and pressures up to 60ÂMPa. Journal of Chemical Thermodynamics, 2020, 147, 106122.	2.0	8
54	Densities and viscosities for binary mixtures of dimethyl carbonate with 1-heptanol, 1-octanol, 1-1 and 1-decanol. Journal of Chemical Thermodynamics, 2021, 157, 106404.	2.0	7

#	Article	IF	CITATIONS
55	Volumetric properties of binary mixtures of methanol with ethyl caprylate, ethyl caprate, and ethyl laurate from 283.15 to 318.15 K. Energy Procedia, 2018, 152, 869-874.	1.8	6
56	Speed of Sound and Derived Properties of Ethyl Nonanoate. Journal of Chemical & Engineering Data, 2019, 64, 3632-3640.	1.9	6
57	Solubilities of R32 in Polyol Ester and Polyvineyl Ether from 278.15 to 348.15 K. Journal of Chemical & Engineering Data, 2020, 65, 4306-4317.	1.9	6
58	Isobaric heat capacity prediction for HC, HFC, HFO and HCFO refrigerants in liquid phase. International Journal of Refrigeration, 2020, 118, 41-49.	3.4	6
59	Solubility behavior of 3, 3, 3-trifluoropropene in 1-hexyl-3-methyl-Imidazolium hexafluorophosphate and 1-octyl-3-methyl-imidazolium hexafluorophosphate. Journal of Molecular Liquids, 2022, 347, 118347.	4.9	6
60	Assessment and development of the viscosity prediction capabilities of entropy scaling method coupled with a modified binary interaction parameter estimation model for refrigerant blends. Journal of Molecular Liquids, 2022, 358, 119184.	4.9	6
61	Gaseous transport properties of hydrogen, deuterium and their binary mixtures from <i>ab initio</i> potential. Molecular Physics, 2013, 111, 49-59.	1.7	5
62	Liquid viscosities of ethyl caprylate and ethyl caprate at elevated temperatures and pressures. Journal of Molecular Liquids, 2020, 309, 113203.	4.9	5
63	Densities and excess molar volumes of the binary system <i>N</i> -methyldiethanolamine + (2-aminoethyl)ethanolamine and its ternary aqueous mixtures from 283.15 to 363.15 K. Physics and Chemistry of Liquids, 2016, 54, 499-506.	1.2	4
64	Accurate virial coefficients of gaseous krypton from state-of-the-art <i>ab initio</i> potential and polarizability of the krypton dimer. Journal of Chemical Physics, 2018, 148, 024306.	3.0	4
65	PÏT measurements and modelling of (n-decane + m-xylene) mixtures from 293.15 K to 363.15 K at pres up to 60 MPa. Journal of Chemical Thermodynamics, 2019, 135, 107-115.	sures 2.0	4
66	Absorption increment of various physical/chemical CO2 absorbents using CeO2/SiO2/TiO2 nanocomposite. Chemical Papers, 2022, 76, 4817-4834.	2.2	4
67	Density and Viscosity Investigation for Binary Mixtures of Polyoxymethylene Dimethyl Ethers with 1-Propanol, 1-Butanol, and 1-Pentanol. Journal of Chemical & Engineering Data, 2022, 67, 334-345.	1.9	3
68	A new semiâ€empirical equation for compressed liquid densities of <i>n</i> â€alkanes. Asia-Pacific Journal of Chemical Engineering, 2013, 8, 425-432.	1.5	2
69	The Eyring's Theory Combined with PR Equation of State and <i>G</i> ^E Mixing Rule for High-Pressure Viscosity Prediction of Binary Liquid Mixtures. Journal of Chemical Engineering of Japan, 2014, 47, 443-451.	0.6	2
70	Measurement of the thermal conductivity of biofuel mixtures: Methyl caprate components of biodiesel and alcohols. Fluid Phase Equilibria, 2019, 501, 112263.	2.5	2
71	Influences of Organic Solvents on the Properties of 1-Butyl-3-methylimidazolium Acetate. Journal of Chemical & Engineering Data, 2020, 65, 1911-1918.	1.9	2
72	High-Pressure Liquid Viscosity of <i>n</i> -Hexadecane/ethyl Octanoate Mixtures. Journal of Chemical & Engineering Data, 2021, 66, 1185-1190.	1.9	2

#	Article	IF	CITATIONS
73	Thermal Conductivity of Pure Noble Gases at Low Density from Ab Initio Prandtl Number. International Journal of Thermophysics, 2013, 34, 402-411.	2.1	1
74	High-pressure densities of n-decane+o-xylene mixtures: Measurement and modelling. Fluid Phase Equilibria, 2019, 498, 1-8.	2.5	1
75	Developing free-volume models for nanofluid viscosity modeling. Journal of Thermal Analysis and Calorimetry, 2022, 147, 777-790.	3.6	1
76	Densities and Viscosities for the Binary Mixtures of n-Nonane with 1-Heptanol, 1-Octanol, 1-Nonanol, and 1-Decanol. Journal of Chemical & Engineering Data, 0, , .	1.9	1
77	Experimental Investigation on Solubility and Viscosity of 1,1,1,2,3,3,3-Heptafluoropropane (R227ea) and Polyol Ester Oil (POE 22) Mixtures. Journal of Chemical & Engineering Data, 2022, 67, 104-112.	1.9	1
78	Liquid Density and Viscosity of Ethyl Caprate/1-Propanol Mixture at High Pressures. Journal of Chemical & Engineering Data, 2022, 67, 1438-1449.	1.9	1
79	Magnetically actuated resonant piezoresistive microcantilever operating in fluid for dc current measurement. , 2013, , .		0
80	Modified Vapor Pressure Model Based on Corresponding-States Principle for Pure and Mixed Refrigerants. Journal of Chemical Engineering of Japan, 2017, 50, 807-814.	0.6	0
81	Determination of the potential energy surfaces of refrigerant mixtures and their gas transport coefficients. Thermal Science, 2017, 21, 2851-2858.	1.1	Ο